Conf-9408182--3

LA-UR- 94-3493

Title: HOT PROTON ANISOTROPIES AND COOL PROTON TEMPERATURES IN THE OUTER MAGNETOSPHERE

Author(s): S. Peter Gary
Mark B. Moldwin
Michelle F. Thomsen
Dan Winske
David J. McComas

Submitted to: Proceedings of the Taos Workshop on the Earth's Trapped Particle Environment

DISCLAIMER

This report was prepared as an account of work sponsored by an agency of the United States Government. Neither the United States Government nor any agency thereof, nor any of their employees, makes any warranty, express or implied, or assumes any legal liability or responsibility for the accuracy, completeness, or usefulness of any information, apparatus, product, or process disclosed, or represents that its use would not infringe privately owned rights. Reference herein to any specific commercial product, process, or service by trade name, trademark, manufacturer, or otherwise does not necessarily constitute or imply its endorsement, recommendation, or favoring by the United States Government or any agency thereof. The views and opinions of authors expressed herein do not necessarily state or reflect those of the United States Government or any agency thereof.

Los Alamos
NATIONAL LABORATORY

Los Alamos National Laboratory, an affirmative action/equal opportunity employer, is operated by the University of California for the U.S. Department of Energy under contract W-7405-ENG-36. By acceptance of this article, the publisher recognizes that the U.S. Government retains a nonexclusive, royalty free license to publish or reproduce the published form of this contribution, or to allow others to do so, for U.S. Government purposes. The Los Alamos National Laboratory requests that the publisher identify this article as work performed under the auspices of the U.S. Department of Energy.

Hot proton anisotropies and cool proton temperatures in the outer magnetosphere

S. Peter Gary, Mark B. Moldwin, Michelle F. Thomsen, Dan Winske, and David J. McComas

Los Alamos National Laboratory, Los Alamos, New Mexico

Abstract. The plasma sheet and ring current ions of the outer magnetosphere typically exhibit an anisotropy such that the perpendicular temperature is greater than the parallel temperature. If such an anisotropy is sufficiently large, the electromagnetic proton cyclotron instability will be excited. This instability is studied using linear Vlasov theory and one-dimensional hybrid simulations for a homogeneous plasma model representative of conditions in the outer magnetosphere. The model includes a hot anisotropic proton component and a cool, initially isotropic proton component. Theory and simulations both predict that there is a threshold hot proton anisotropy for this instability which depends inversely on the parallel β of the hot component. The simulations are also used to examine the nonlinear response of the cool protons to the proton cyclotron instability; the late-time temperature of the cool protons is found to increase as the relative hot proton density increases. Analysis of plasma observations obtained by the Los Alamos magnetospheric plasma analyzer in geosynchronous orbit finds that the hot ion anisotropy is indeed bounded by the predicted β-dependent threshold.

1. Introduction

The recent increase in the use of statistical methods for the analysis of spacecraft data has led to the discovery of several correlations between or among observed plasma parameters in and near the terrestrial magnetosphere. It is important to understand these correlations because they can provide constraints on, and thereby improve the accuracy and predictive capability of, large-scale magnetohydrodynamic (MHD) models of the magnetosphere.

Some of these correlations may reflect plasma response to the large-scale dynamics of the magnetosphere, and in such cases it is appropriate to interpret them in terms of MHD theories. For example, recent studies of the statistical relationship between pressure and density as observed in the geomagnetic tail have been examined in terms of an MHD framework [see *Goertz and Baumjohann*, 1991, and references therein]. However, other observed correlations may be due to small-scale, kinetic processes, and therefore require interpretation in terms of Vlasov theory and particle simulations.

An example of a statistical relationship which is induced by kinetic plasma physics is the inverse correlation between the proton temperature anisotropy and the proton parallel β in the highly compressed terrestrial magnetosheath discovered by *Anderson et al.* [1994] and which takes the form

$$\frac{T_{\perp p}}{T_{\parallel p}} - 1 = \frac{0.85}{\beta_{\parallel p}^{0.48}} \qquad (1)$$

where the perpendicular and parallel symbols denote directions relative to the background magnetic field $\mathbf{B}_o$ and $\beta_{\parallel p} \equiv 8\pi n_p T_{\parallel p}/B_o^2$. Linear Vlasov theory has been used to show that such a relationship corresponds to the threshold condition of the electromagnetic proton cyclotron anisotropy instability [*Gary and Lee*, 1994]; hybrid simulations of this instability have further demonstrated that such a relation represents an upper bound on $T_{\perp p}/T_{\parallel p}$ [*Gary et al.*, 1994a]. Although the numerical values of the coefficients on the right-hand side of (1) vary with the choice of maximum linear growth rate at threshold and on the presence of other ionic species [*Gary et al.*, 1993a, b], these variations are relatively weak for magnetosheath parameters so that several different sheath observations have yielded similar upper bounds [*Hau et al.*, 1993; *Phan et al.*, 1994; *Fuselier et al.*, 1994].

Gary et al. [1994b] has argued that a related anisotropy upper bound may be observed in the outer magnetosphere. Measurements at geosynchronous orbit typically show the coexistence of hot and cool ion components [e.g., *McComas et al.*, 1993]. The hot component, termed plasma sheet or ring current ions, typically has a plasma temperature of several keV and is usually anisotropic ($T_\perp/T_\parallel > 1$) and relatively tenuous ($n \lesssim 1$ cm^{-3}) [*Mauk and McPherron*, 1980; *Anderson and Hamilton*, 1993]. The cool ion component is usually identified as consisting of one of two types. Plasma trough ions are much cooler (1 to 10 eV) but more dense ($n \sim 1$ to 10 cm^{-3}) than the hot component, whereas plasmaspheric ions are still cooler (of order 1 eV) and still more dense ($n \sim 10$ to 100 cm^{-3}) [*Reasoner et al.*, 1983]. *Gary et al.* [1994b] represented these conditions with a hot proton/cool proton model, and showed that, in this model, the electromagnetic proton cyclotron anisotropy instability (hereafter the "proton cyclotron instability") leads to an upper bound on the hot proton anisotropy and furthermore implies a scaling for the temperature of the cool proton component.

If the ion distribution functions of a plasma are approximately bi-Maxwellian with $T_{\perp i} > T_{\parallel i}$, then several instabilities driven by such anisotropies may arise. In an electron/proton plasma with $T_{\perp p} > T_{\parallel p}$ and $\beta_{\parallel p} \lesssim 1$ the growing mode of lowest threshold is the proton cyclotron instability [*Gary et al.*, 1976]. Linear Vlasov theory in a homogeneous, collisionless plasma predicts that this instability grows at real frequencies ω_r less than Ω_p, the proton cyclotron frequency, with maximum growth rate γ_m at propagation strictly parallel to $\mathbf{B}_o$, and with strictly transverse electromagnetic fluctuations ($\delta\mathbf{B}$ and $\delta\mathbf{E}$ perpendicular to $\mathbf{B}_o$) [*Gary*, 1993, and references therein]. We term transverse fluctuations in the range $\Omega_{He+} < \omega_r < \Omega_p$ "proton-cyclotron-like" fluctuations.

Equation (1) corresponds to a threshold of the proton cyclotron instability, and, as such, represents an upper bound on the proton temperature anisotropy. If the anisotropy is less than the threshold value, there is no significant instability growth, no wave-particle scattering, and no local change in $T_{\perp p}/T_{\parallel p}$. On the other hand, if the plasma is driven by macroscopic forces such that $T_{\perp p}/T_{\parallel p}$ exceeds the threshold

condition for a given $\beta_{\|p}$, the proton cyclotron instability will arise and will pitch angle scatter the protons. If the convection of fluctuation energy away from the region of excitation is not too rapid, this scattering will return the anisotropy to threshold.

This interpretation of (1) implies that a relationship of this form should be observed not only in the magnetosheath but also in any collisionless, sufficiently homogeneous plasma in which the proton cyclotron instability is excited. Because $T_\perp/T_\| > 1$ is a prevailing condition for protons in the outer magnetosphere, and because proton-cyclotron-like fluctuations are often observed in the terrestrial magnetosphere, especially at geosynchronous orbit and beyond [*Mauk and McPherron*, 1980; *Young et al.*, 1981; *Fraser*, 1985; *Anderson et al.*, 1992], it is likely that an upper bound similar to (1) should be observable there.

To represent outer magnetospheric conditions, we assume that there are only two species present, protons (denoted by subscript p) and electrons (subscript e), but that there are two proton components: the anisotropic hot component (subscript h) and the initially isotropic cool component (subscript c). We assume that each component is represented by a bi-Maxwellian for both the zeroth-order distribution functions of linear theory and the initial proton distribution functions of the simulations.

Table 1 states the values of the dimensionless parameters which we use in both our linear theory and simulations; in particular, we assume the electrons and the cool proton component are initially isotropic, and choose $T_{\|c} = 0.001 T_{\|h}$ and $T_e = (n_c T_{\|c} + n_h T_{\|h})/n_e$. We consider only $\mathbf{k} \times \mathbf{B}_o = 0$, corresponding to the direction of propagation which yields the maximum growth rate. The linear theory properties of the proton cyclotron instability at propagation parallel to $\mathbf{B}_o$ are essentially independent of the electron temperature, so our choice of electron temperature and our neglect of the hot/cool two component nature of magnetospheric electrons are valid approximations for the work described below. Charge neutrality is satisfied ($\sum_j c_j n_j = 0$ where the sum is over both species and both proton components).

The notation of this manuscript is the same as in *Gary et al.* [1994b]. We assume that the hot proton anisotropy at instability threshold may be written in the form

$$\frac{T_{\perp h}}{T_{\|h}} - 1 = \frac{S_h'}{\beta_{\|h}^{\alpha_h}} \qquad (2)$$

2. Linear Theory

Numerical solutions of the full linear Vlasov dispersion equation for the parameters given in Table 1 show that there are two instabilities that can be driven by $T_{\perp h}/T_{\|h} > 1$. These are the proton cyclotron instability and the mirror instability [see, for example, *Gary*, 1993]. Figure 1 compares the threshold for the two growing modes and shows that, for the usual magnetospheric condition of $\beta_{\|h} \lesssim 1$, the former instability has the lower threshold. This statement is

true not only for the choice $n_h/n_e = 0.50$ used in Figure 1, but for a wide range of hot proton relative densities, so that we concentrate on the proton cyclotron instability in the following discussion.

The second point illustrated by Figure 1 is the power law relationship between the proton temperature anisotropy and $\beta_{\parallel h}$ at a fixed value of the maximum growth rate. For the parameters of Figure 1 we have $\alpha_h = 0.42$. This value is similar not only to many other determinations of α_h from linear theory and computer simulations [e.g., *Gary et al.*, 1994b], but also to the power of $\beta_{\parallel p}$ in the observed result of Equation (1).

Fig. 3 of *Gary et al.* [1994b] shows that, as long as $T_{\parallel c}/T_{\parallel h} \lesssim 0.1$, variations in the cool proton temperature do not affect the threshold significantly. Similar sample computations at $n_h/n_e = 0.10$ and $\beta_{\parallel h} = 0.10$ demonstrate no important changes in the hot proton temperature anisotropy at instability threshold over the range $0.10 \leq T_{\perp c}/T_{\parallel c} \leq 10.0$. Therefore S_h'' of Equation (2) is essentially independent of the thermal properties of the cool protons. However, this quantity does depend on the hot proton relative density. In particular, *Gary et al.* [1994b] showed that, at sufficiently large values of n_h/n_e and sufficiently small values of γ_m/Ω_p, S_h'' is proportional to $(n_h/n_e)^{M_h}$. Here we consider the complementary case of $0.001 \leq n_h/n_e \leq 0.10$ where, for $\gamma_m/\Omega_p \simeq 0.005$, the hot proton anisotropy is relatively independent of the hot proton relative density (for example, see Fig. 2 of *Gary et al.*, 1994). Then at $\beta_{\parallel h} = 0.10$ linear theory implies $S_h'' \simeq 0.29$ at $\gamma_m/\Omega_p = 0.005$ and $S_h'' \simeq 0.18$ at $\gamma_m/\Omega_p = 0.002$.

3. Simulations

This section describes results from simulations of the proton cyclotron instability using the same two-component proton model utilized in the previous section. The computations use the one-dimensional hybrid code of *Winske and Omidi* [1993], which has been used many times to simulate this instability under conditions appropriate to the terrestrial magnetosheath [*Gary et al.*, 1994a, and references therein]. In a hybrid simulation the protons are represented as collisionless superparticles and the electrons are taken as a massless fluid. This is an appropriate model for this instability because the hot protons are resonant ($1 \lesssim |\zeta_h^-| \lesssim 3$) with this instability, whereas the electrons are nonresonant ($|\zeta_e^{\pm}| >> 1$). All computations described here are initial value simulations carried out with periodic boundary conditions at $\mathbf{k} \times \mathbf{B}_o = 0$, and with the following parameters: 128 cells, an integration time step of $\Delta t \Omega_p = 0.05$, 12800 hot superparticles and 6400 cool superparticles. The superparticles of each component are weighted so that the relative densities they represent may be changed without changing the number of superparticles themselves. We choose the system length so that mode 8 (the mode with eight wavelengths within the simulation box) approximately corresponds to the wavelength of maximum growth rate. This permits the

simulation to represent a broadband spectrum of growing fluctuations for all parameter ranges considered here.

There have been several self-consistent simulations of the proton cyclotron instability in the presence of a cool ionic component [*Cuperman and Sternlieb*, 1977; *Cuperman*, 1981; *Tanaka*, 1985; *Omura et al.*, 1985; *Machida et al.*, 1988]. Such simulations typically demonstrate that the fluctuating fields attain a relatively weak maximum amplitude ($|\delta B|^2 << B_o^2$) and that the saturation mechanism is hot proton pitch angle scattering which acts over a relatively wide range of proton parallel velocities to reduce $T_{\perp h}/T_{\parallel h}$ to the condition of weak growth or stability. The addition of cool ions to the simulations enhances the magnetic fluctuation energy at saturation [*Cuperman and Sternlieb*, 1977] and leads to strong heating of the cool component if that component is cyclotron resonant with the instability [*Tanaka*, 1985]. *Omura et al.* [1985] also found that, because they are nonresonant, cool protons were heated much less strongly than cool helium ions.

Figure 2 shows results from a representative simulation of the proton cyclotron instability in our model. Here $n_h/n_e = 0.10$, and the initial values of the dimensionless parameters are as given in Table 1 with $\beta_{\parallel h} = 0.10$ and $T_{\perp h}/T_{\parallel h} = 6.07$, which yield an initial linear growth rate of $\gamma_m = 0.10\Omega_p$. As in many other self-consistent calculations of this instability, the fluctuating magnetic field grows rapidly to saturation at a relatively low level. Wave-particle scattering by the enhanced fluctuations reduces $T_{\perp h}$ (not shown) and increases $T_{\parallel h}$, just as in simulations in which only a single proton component is present [e.g., *McKean et al.* 1992], so that the temperature anisotropy of the hot protons attains a slowly changing late-time condition.

Figure 3 presents late-time results for the hot proton temperature anisotropy from four ensembles of simulations corresponding to four different initial values of γ_m/Ω_p. Here $n_h/n_e = 0.10$ and all other dimensionless variables except for the hot proton temperature anisotropy and $\beta_{\parallel h}$ were initially chosen as described in Table 1. Then, for each choice of initial values for $\beta_{\parallel h}$ and γ_m/Ω_p, for each run $T_{\perp h}/T_{\parallel h}$ was chosen to satisfy the condition of constant initial growth rate.

Figure 3 shows that the late-time hot proton temperature anisotropy for each ensemble well satisfies the $\beta_{\parallel h}$-dependence of Equation (2), and that α_h is relatively independent of the choice of initial value of γ_m/Ω_p. The results here are commensurate with the average value $\alpha_h = 0.41$ stated by *Gary et al.* [1994b]. In contrast $T_{\perp h}/T_{\parallel h} - 1$ does not generally satisfy a power law dependence on n_h/n_e, but rather exhibits the same type of nonmonotonic response to the hot proton relative density in the simulations as it does at thresholds determined from linear theory [*Gary et al.*, 1994b, Figs. 2 and 7].

The cool protons are nonresonant with respect to the proton cyclotron instability, that is, $|\zeta_c| >> 1$. The cool proton response shown in Figure 2 is the relatively weak heating expected for such a component, and is characteristic of many of our computations. At early times $T_{\perp c}$ (not shown) and $T_{\perp c}/T_{\parallel c}$ increase rapidly, reaching maximum values at

about the same time as $|\delta B|^2/B_o^2$ reaches saturation. At later times there is a more gradual increase of $T_{\|c}$ with a commensurate gradual reduction of $T_{\perp c}$; as shown in Figure 2b the cool proton average temperature T_c strikes a balance between these two trends and attains a relatively constant value at late times. Because this is true of many of our simulations, we chose $T_c/T_{\|h}$ as the dimensionless variable characterizing the cool proton response in our simulations. The overall increase in T_c is no lest, in agreement with the simulations of *Omura et al.* [1985].

Results from *Gary et al.* [1994b] showed no significant change with $T_c(0)/T_{\|h}(0)$ in either $|\delta B|^2/B_o^2$ at saturation or $T_{\perp h}/T_{\|h}$ at late times, demonstrating that not only the hot proton anisotropy but also the maximum fluctuating field amplitude is essentially independent of the cool proton average temperature. Under the assumption that the late-time $T_c/T_{\|h}$ is independent of the initial choice of $T_{\|c}/T_{\|h}$ if the value of the latter is sufficiently small, we seek a scaling relation of the form

$$\frac{T_c}{T_{\|h}} = \frac{S_c}{\mathcal{A}_{\|h}^{\alpha_c}} \left(\frac{n_h}{n_c}\right)^{M_c} \tag{3}$$

Figure 4 plots $T_c/T_{\|h}$ results from simulations of the proton cyclotron instability as a function of the hot/cool proton relative density. Here the four ensembles correspond to a range of n_h/n_c values for four different initial values of the maximum growth rate. Here both temperatures are evaluated at the time of maximum T_c, which in most simulations is approximately the time of maximum fluctuating magnetic field amplitude. Although the slope variation is somewhat greater than in Figure 3, extrapolation of the results here to the limit of zero growth rate yields $M_c = 0.37$. If we plot $T_c/T_{\|h}$ at maximum value of T_c as a function of $\mathcal{A}_{\|h}$ from the ensemble of simulations corresponding to Figure 3, we find that α_c has substantial variation with $\gamma_m(0)/\Omega_p$; although there is no clear small growth rate limit, we choose $\alpha_c \simeq 0$. To determine the last factor on the right-hand side of Equation (3) we choose $\gamma_m(0)/\Omega_p = 0.01$; this implies $S_c = 0.009$.

4. Observations

Our analysis uses data from the Los Alamos National Laboratory magnetospheric plasma analyzer (MPA) onboard the geosynchronous spacecraft 1989-046. A complete description of the instrument is given in *Bame et al.*, [1993], and examples of the plasma data are shown in *McComas et al.* [1993]. The MPA does not distinguish between protons and heavier ions, so for the purpose of our analysis we assume that both hot and cool observed ion components are protons.

As in *Gary et al.* [1994b], we have examined data from two eleven-day intervals, November 11-20, 1993 and January 21-31, 1994, chosen because of their relatively low backgrounds. We here present results only from the latter

interval, although results from the former interval are similar. Because this spacecraft does not carry a magnetometer, we estimate B_o from the Tsyganenko model for relatively quiet magnetospheric conditions. We use an approximate fit to this model of the form

$$B_o = 100 - 15\cos(2\pi\tau_{LT}/24.0) \qquad (4)$$

where τ_{LT} is the local time in decimal hours and B_o is the value of the magnetic field at synchronous orbit in nanoteslas.

To compare the data against theory, we use a somewhat different approach than that of *Gary et al.* [1994b]. We have plotted n_h/n_e as a function of S'_h for our two eleven-day intervals; the results show that at $0.001 \leq n_h/n_e \leq 0.10$ these two parameters are essentially uncorrelated. As we have discussed in Section 2, linear Vlasov theory predicts that the hot proton anisotropy should be relatively independent of n_h/n_e in this regime. Therefore, we may compare the data against the theoretical form of Equation (2) where S'_h for growth rates of interest is as stated in Section 2. Observations and theory are compared in Figure 5. The observed points are for the most part bounded by the line corresponding to $\gamma_m/\Omega_p = 0.005$, and appear to cluster somewhat above the line corresponding to $\gamma_m/\Omega_p = 0.002$. Therefore, for this interval, the hot proton anisotropy has an approximate upper bound that corresponds to a maximum growth rate of the proton cyclotron instability $\gamma_m \lesssim 5 \times 10^{-3}\Omega_p$. We conclude that this value of γ_m represents the average maximum growth rate value necessary to maintain the hot proton temperature anisotropy at an upper bound against the large-scale magnetospheric forces acting to increase $T_{\perp h}/T_{\parallel h}$.

At the time of the writing of this manuscript the algorithms for the reduction of the cool ion moments from the MPA data are undergoing refinement. Thus the T_c observations presented as Fig. 10 of *Gary et al.* [1994b] must be regarded as preliminary, and it is not yet appropriate to carry out a detailed observational comparison against the predicted form of Equation (3). However we can make two qualitative statements. First, theory and simulations predict that cool proton heating by the proton cyclotron instability is a nonresonant process, which is in agreement with the recent observations of *Anderson and Fuselier* [1994]. Second, because our analysis shows that n_h and $T_{\parallel h}$ have relatively small variations over the eleven-day data sets we have chosen, Equation (3) predicts an inverse correlation between T_c and r_c, in agreement with the observations of *Moldwin et al.* [1994].

5. Conclusions

Gary et al. [1994b] have used linear Vlasov theory and one-dimensional hybrid simulations to study the consequences of scattering by enhanced fluctuations from the electromagnetic proton cyclotron anisotropy instability. Our outer magnetospheric model assumes a homogeneous plasma with a hot, anisotropic proton component and a

cool, initially isotropic proton component. From this model we obtain scalings for the upper bound on the temperature anisotropy of the hot protons and for the cool/hot temperature ratio, as functions of $\beta_{\parallel h}$ and the hot proton relative density. Analysis of data from Los Alamos plasma instruments at geosynchronous orbit shows general agreement with the theoretical scaling relation for $T_{\perp h}/T_{\parallel h}$. This agreement provides evidence that the proton cyclotron instability is acting in the outer magnetosphere to limit the hot proton anisotropy. We believe that this hot proton anisotropy upper bound can be useful not only as a limited closure relation for macroscopic models of magnetospheric plasmas, but also for determining plasma conditions in magnetospheric wave propagation calculations (e.g., as a replacement for the constant anisotropy condition used by *Horne and Thorne* [1993] and others.).

Acknowledgments. The authors acknowledge useful exchanges with Brian Anderson, Richard Denton, Steve Fuselier, and Song Xue. This work was performed under the auspices of the U.S. Department of Energy (DOE) and was supported by the DOE Office of Basic Energy Sciences, Division of Engineering and Geosciences, and both the SR&T Program and the Space Plasma Theory Program of the National Aeronautics and Space Administration (NASA).

Table 1. Dimensionless Parameter Model

Parameter	Hot Protons	Cool Protons	Electrons
m_j/m_p	1.0	1.0	1/1836
c_j/c_p	1.0	1.0	−1.0
n_j/n_e	Variable	$1 - n_h/n_e$	1.00
$T_{\parallel j}/T_{\parallel h}$	1.0	0.0001	$n_h/n_e + n_c/n_e(T_{\parallel c}/T_{\parallel h})$
$T_{\perp j}/T_{\parallel j}$	Variable	1.0	1.0

$v_A/c = 1 \times 10^{-3}$

References

Anderson, B. J., and S. A. Fuselier, Response of thermal ions to electromagnetic ion cyclotron waves, *J. Geophys. Res.*, *99*, 19,413, 1994.

Anderson, B. J., and D. C. Hamilton, Electromagnetic ion cyclotron waves stimulated by modest magnetospheric compressions, *J. Geophys. Res.*, *98*, 11,369, 1993.

Anderson, B. J., R. E. Erlandson, and L.J. Zanetti, A statistical study of Pc 1-2 magnetic pulsations in the equatorial magnetosphere, 1. Equatorial occurrence distributions, *J. Geophys. Res.*, *97*, 3075, 1992.

Anderson, B. J., S. A. Fuselier, S. P. Gary and R. E. Denton, Magnetic spectral signatures in the Earth's magnetosheath and plasma depletion layer, *J. Geophys. Res.*, *99*, 5877, 1994.

Bame, S. J., D. J. McComas, M. F. Thomsen, B. L. Barraclough, R. C. Elphic, J. P. Glore, J. T. Gosling, J. C. Chavez, E. P. Evans, and F. J. Wymer, Magnetospheric

plasma analyzer for spacecraft with constrained resources, *Rev. Sci. Instrum.*, *64*, 1026, 1993.

Cuperman, S., Electromagnetic kinetic instabilities in multicomponent space plasmas: Theoretical predictions and computer simulation experiments, *Rev. Geophys.*, *19*, 307, 1981.

Cuperman, S., and A. Sternlieb, Numerical-experimental investigation of the enhancement of the electromagnetic ion cyclotron instability by cold plasma, *J. Geophys. Res.*, *82*, 181, 1977.

Fraser, B. J., Observations of ion cyclotron waves near synchronous orbit and on the ground, *Space Sci. Rev.*, *42*, 357, 1985.

Fuselier, S. A., B. J. Anderson, S. P. Gary, and R. E. Denton, Inverse correlations between the ion temperature anisotropy and plasma beta in the Earth's quasi-parallel magnetosheath, *J. Geophys. Res.*, *99*, 14,931, 1994.

Gary, S. P., *Theory of Space Plasma Microinstabilities*, Cambridge University Press, Cambridge, 1993.

Gary, S. P., and M. A. Lee, The ion cyclotron instability and the inverse correlation between proton anisotropy and proton beta, *J. Geophys. Res.*, *99*, 11,297, 1994.

Gary, S. P., M. D. Montgomery, W. C. Feldman, and D. W. Forslund, Proton temperature anisotropy instabilities in the solar wind, *J. Geophys. Res.*, *81*, 1241, 1976.

Gary, S. P., S. A. Fuselier, and B. J. Anderson, Ion anisotropy instabilities in the magnetosheath, *J. Geophys. Res.*, *98*, 1481, 1993a.

Gary, S. P., M. E. McKean, and E. Winske, Ion cyclotron anisotropy instabilities in the magnetosheath: Theory and simulations, *J. Geophys. Res.*, *98*, 3963, 1993b.

Gary, S. P., M. E. McKean, D. Winske, B. J. Anderson, R. E. Denton, and S. A. Fuselier, The proton cyclotron instability and the anisotropy/β inverse correlation, *J. Geophys. Res.*, *99*, 5903, 1994a.

Gary, S. P., M. B. Moldwin, M. F. Thomsen, D. Winske, and D. J. McComas, Hot proton anisotropies and cool proton temperatures in the outer magnetosphere, *J. Geophys. Res.*, **99**, xxxxx, 1994b.

Goertz, C. K., and W. Baumjohann, On the thermodynamics of the plasma sheet, *J. Geophys. Res.*, *96*, 20,991, 1991.

Hau, L.-N., T.-D. Phan, B. U. Ö. Sonnerup, and G. Paschmann, Double-polytropic closure in the magnetosheath, *Geophys. Res. Lett.*, *20*, 2255, 1993.

Horne, R. B., and R. M. Thorne, On the preferred source location for the convective amplification of ion cyclotron waves, *J. Geophys. Res.*, *98*, 9233, 1993.

Machida, S., C. K. Goertz, and T. Hada, The electromagnetic ion cyclotron instability in the Io torus, *J. Geophys. Res.*, *93*, 7545, 1988.

Mauk, B. H., and R. L. McPherron, An experimental test of the electromagnetic ion cyclotron instability within the earth's magnetosphere, *Phys. Fluids*, *23*, 2111, 1980.

McComas, D. J., S. J. Bame, B. L. Barraclough, J. R. Donart, R. C. Elphic, J. T. Gosling, M. B. Moldwin, K. R.

Moore, and M. F. Thomsen, Magnetospheric plasma analyzer: Initial three-spacecraft observations from geosynchronous orbit, *J. Geophys. Res.*, *98*, 13,453, 1993.

McKean, M. E., D. Winske, and S. P. Gary, Mirror and ion cyclotron anisotropy instabilities in the magnetosheath, *J. Geophys. Res.*, *97*, 19,421, 1992.

Moldwin, M. B., M. F. Thomsen, S. J. Bame, D. J. McComas, and K. R. Moore, The structure and dynamics of the outer plasmasphere: A multiple geosynchronous satellite study, *J. Geophys. Res.*, *99*, 11,475, 1994.

Omura, Y., M. Ashour-Abdalla, R. Gendrin, and K. Quest, Heating of thermal helium in the equatorial magnetosphere: a simulation study, *J. Geophys. Res.*, *90*, 8281, 1985.

Phan, T.-D., G. Paschmann, W. Baumjohann, and N. Sckopke, The magnetosheath region adjacent to the dayside magnetopause: AMPTE/IRM observations, *J. Geophys. Res.*, *99*, 121, 1994.

Reasoner, D. L., P. D. Craven, and C. R. Chappell, Characteristics of low-energy plasma in the plasmasphere and plasma trough, *J. Geophys. Res.*, *88*, 7913, 1983.

Tanaka, M., Simulations of heavy ion heating by electromagnetic ion cyclotron waves driven by proton temperature anisotropies, *J. Geophys. Res.*, *90*, 6459, 1985.

Winske, D., and N. Omidi, Hybrid codes: Methods and applications, in *Computer Space Plasma Physics: Simulation Techniques and Software*, edited by H. Matsumoto and Y. Omura, p. 103, Terra Scientific, Tokyo, 1993.

Young, D. T., S. Perraut, A. Roux, C. de Villedary, R. Gendrin, A. Korth, G. Kremser, and D. Jones, Wave-particle interactions near Ω_{He^+} observed on GEOS 1 and 2. 1. Propagation of ion cyclotron waves in He^+-rich plasma, *J. Geophys. Res.*, *86*, 6755, 1981.

S. P. Gary, D. J. McComas, M. B. Moldwin, and M. F. Thomsen, M. S. D466, Los Alamos National Laboratory, Los Alamos, NM 87545 (Internet: pgary@lanl.gov, dmccomas@lanl.gov, mmoldwin@lanl.gov, mthomsen@lanl.gov)

D. Winske, M. S. F645, Los Alamos National Laboratory, Los Alamos, NM 87545 (Internet: dw@demos.lanl.gov)

Figure 1. The hot proton temperature anisotropy at the $\gamma_m = 0.01\Omega_p$ threshold of the proton cyclotron instability and the mirror instability determined from linear Vlasov theory as a function of the parallel hot proton β. Here $n_h/n_e = 0.50$; other parameters are as given in Table 1. The individual points are computed from the linear dispersion equation; the corresponding lines are least-squares fits to the points with $\alpha_h = 0.42$ for the proton cyclotron instability and $\alpha_h = 0.58$ for the mirror instability.

Figure 2. Results as a function of time from a representative simulation of the proton cyclotron instability. The

initial values of the dimensionless parameters are as given in Table 1 (except in this case we used an initial value of $T_c = 0.001 T_{\|h}$), with $n_h/n_e = 0.10$, $\beta_{\|h} = 0.10$, and $T_{\perp h}/T_{\|h} = 6.07$, corresponding to an initial $\gamma_m = 0.10\Omega_p$. (a) The solid dots represent the temperature anisotropy of the hot proton component, the solid squares represent the temperature anisotropy of the cool proton component, and the crosses represent the parallel temperature of the hot protons normalized to the initial value of that parameter. (b) The square dots represent the parallel temperature of the cool protons normalized to the initial value of the parallel hot proton temperature, and the open squares represent the total fluctuating magnetic field energy density normalized to the energy density of the background magnetic field [From *Gary et al.*, 1994b].

Figure 3. Late-time values of the proton temperature anisotropy as a function of the late-time proton parallel β with $n_h/n_e = 0.10$ from simulations of the proton cyclotron instability using initial parameters as given in Table 1. The solid dots correspond to runs with $\gamma_m(0)/\Omega_p = 0.10$, the open squares correspond to runs with $\gamma_m(0)/\Omega_p = 0.05$, the open triangles correspond to runs with $\gamma_m(0)/\Omega_p = 0.02$, and the open diamonds correspond to runs with $\gamma_m(0)/\Omega_p = 0.01$. Here each point is obtained by averaging over five results from near the end of each simulation, where the runs go to $\Omega_p t = 200$ for $\gamma_m(0)/\Omega_p = 0.10$ and 0.05, $\Omega_p t = 400$ for $\gamma_m(0)/\Omega_p = 0.02$, and $\Omega_p t = 600$ for $\gamma_m(0)/\Omega_p = 0.01$. The lines represent least-squares fits to each ensemble; these fits yield $\alpha_h = 0.40$ for $\gamma_m(0)/\Omega_p = 0.10$, $\alpha_h = 0.49$ for $\gamma_m(0)/\Omega_p = 0.05$, $\alpha_h = 0.48$ for $\gamma_m(0)/\Omega_p = 0.02$, and $\alpha_h = 0.51$ for $\gamma_m(0)/\Omega_p = 0.01$.

Figure 4. The dimensionless cool proton temperature at the maximum value of T_c as a function of the hot/cool proton relative density from simulations of the proton cyclotron instability using initial parameters as given in Table 1 and *betaparallelh*$(0) = 0.10$. The solid dots correspond to runs with $\gamma_m(0)/\Omega_p = 0.10$, the open squares correspond to runs with $\gamma_m(0)/\Omega_p = 0.05$, the open triangles correspond to runs with $\gamma_m(0)/\Omega_p = 0.02$, and the open diamonds correspond to runs with $\gamma_m(0)/\Omega_p = 0.01$. The lines represent least-squares fits to each ensemble; these fits yield $M_c = 1.18$ for $\gamma_m(0)/\Omega_p = 0.10$, $M_c = 1.01$ for $\gamma_m(0)/\Omega_p = 0.05$, $M_c = 0.90$ for $\gamma_m(0)/\Omega_p = 0.02$, and $M_c = 0.83$ for $\gamma_m(0)/\Omega_p = 0.01$.

Figure 5. The hot proton temperature anisotropy as a function of $\beta_{\|h}$ using the geosynchronous orbit data set described in *Gary et al.* [1994b] for $0.001 \leq n_h/n_e \leq 0.10$. The individual points correspond to data from January 21-31, 1994. The two lines represent Equation (2) with $\alpha_h = 0.44$. The solid line corresponds to $S'_h = 0.29$, which is obtained from a maximum growth rate of $\gamma_m/\Omega_p = 0.005$, whereas the dashed line corresponds to $S'_h = 0.18$, which is obtained from a maximum growth rate of $\gamma_m/\Omega_p = 0.002$.

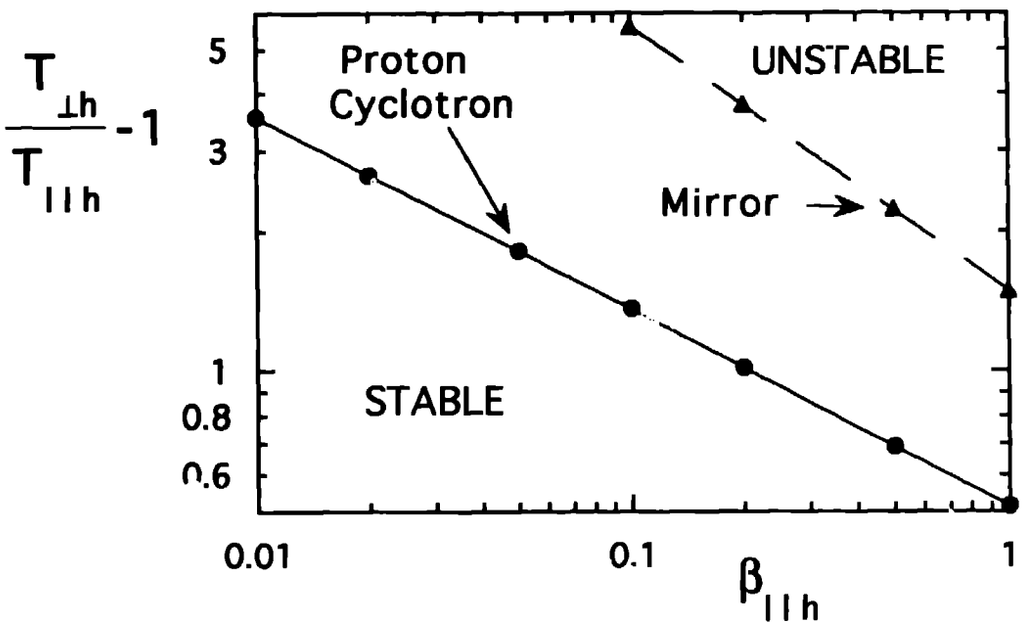
$\frac{T_{\perp h}}{T_{\parallel h}} - 1$
5
3
1
0.8
0.6
Proton
Cyclotron
UNSTABLE
Mirror
STABLE
0.01
0.1
1
$\beta_{\parallel h}$

Figure 1

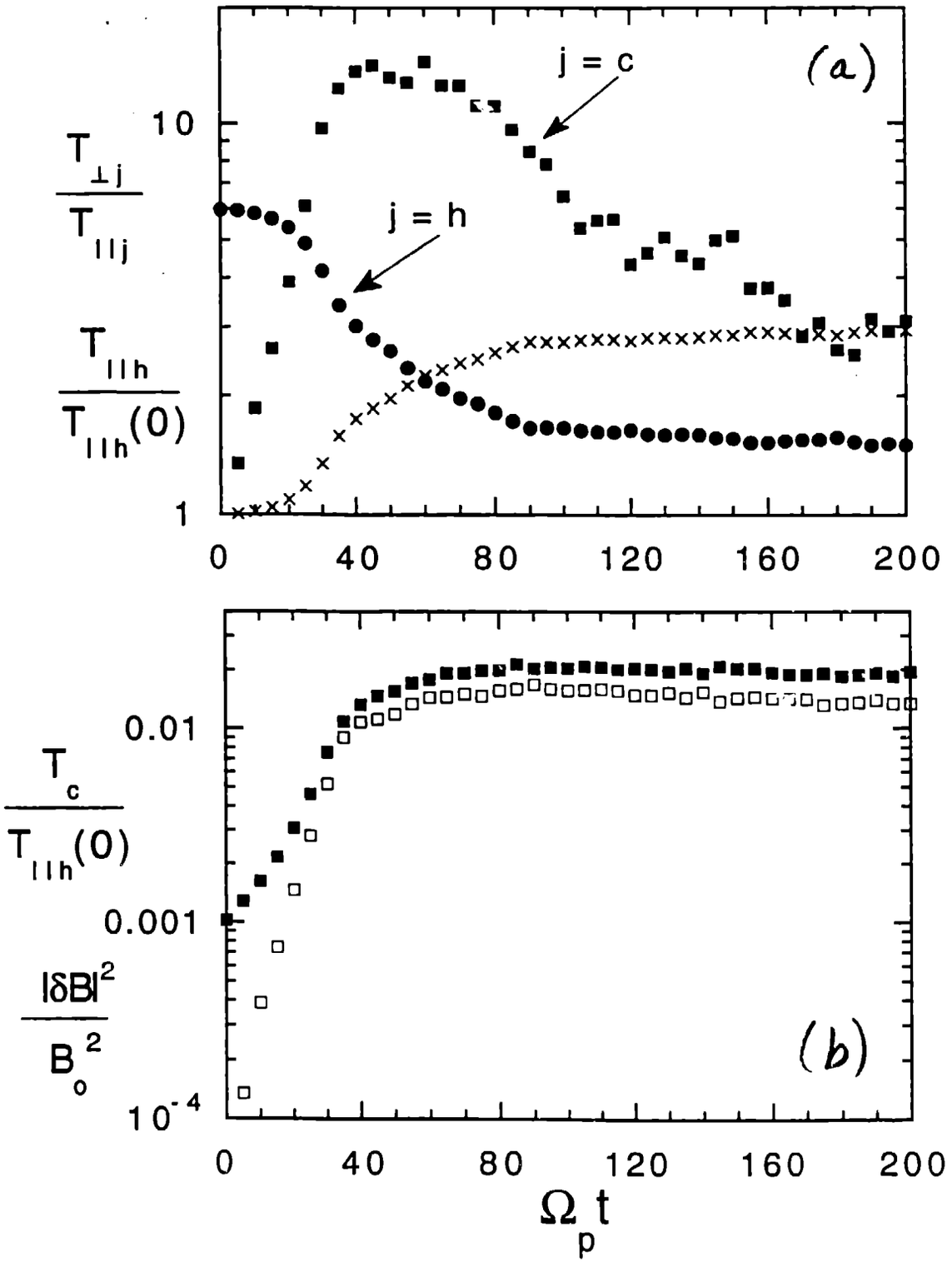
j = c
(a)
j = h
$\frac{T_{\perp j}}{T_{\parallel j}}$
$\frac{T_{\parallel h}}{T_{\parallel h}(0)}$
10
1
0
40
80
120
160
200
$\frac{T_c}{T_{\parallel h}(0)}$
$\frac{|\delta B|^2}{B_o^2}$
0.01
0.001
10^{-4}
(b)
$\Omega_p t$

Figure 2

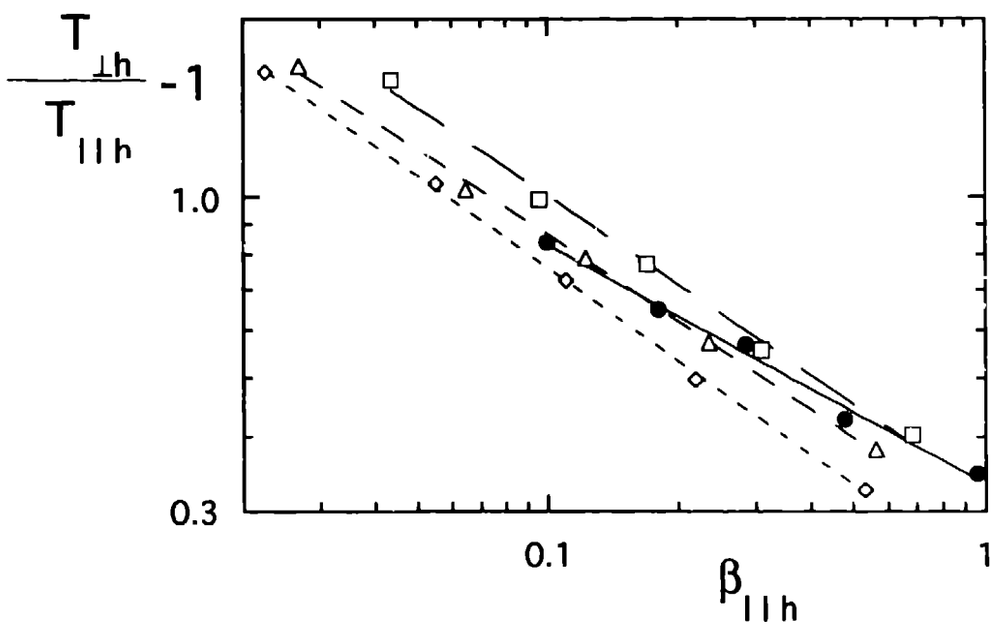

Figure 3

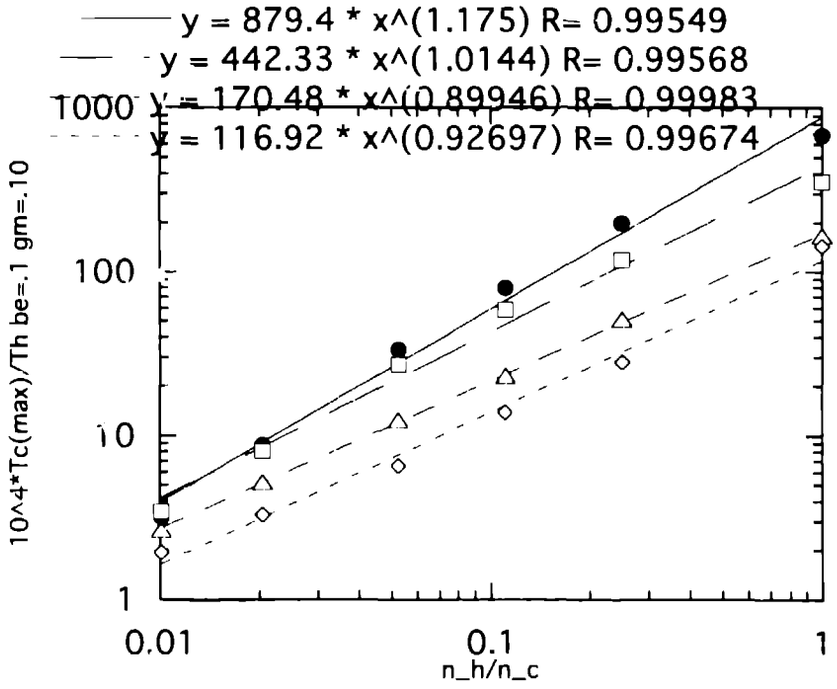
y = 879.4 * x^(1.175) R= 0.99549
y = 442.33 * x^(1.0144) R= 0.99568
y = 170.48 * x^(0.89946) R= 0.99983
y = 116.92 * x^(0.92697) R= 0.99674
1000
100
10
1
10^4*Tc(max)/Th be=.1 gm=.10
0.01
0.1
1
n_h/n_c

Figure 4

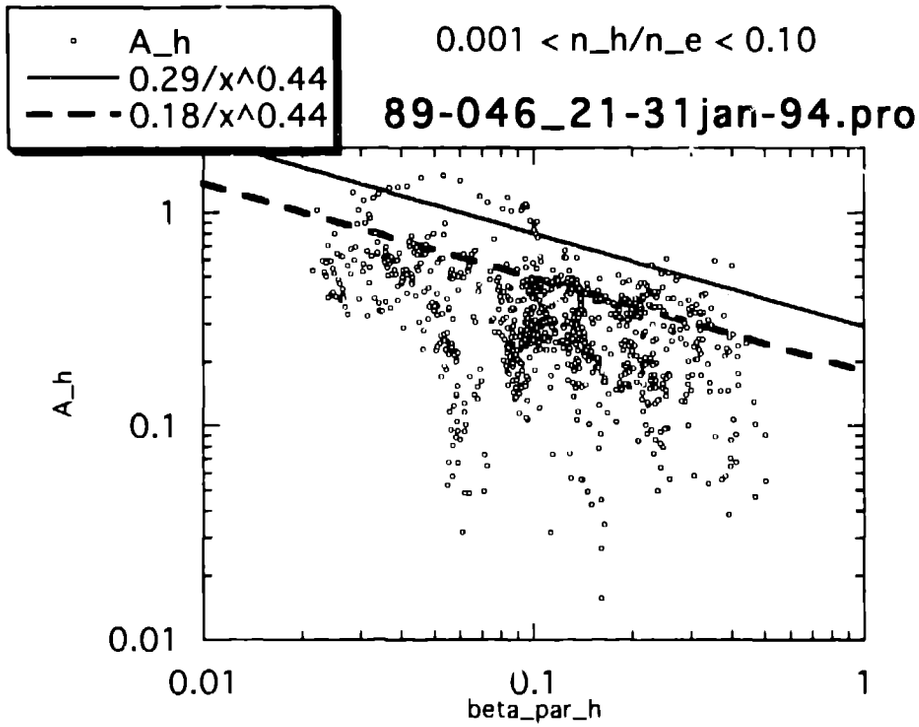
A_h
0.29/x^0.44
0.18/x^0.44
0.001 < n_h/n_e < 0.10
89-046_21-31jan-94.pro
A_h
1
0.1
0.01
0.01
0.1
1
beta_par_h

Figure 5